JOURNAL OF NEUROTRAUMA 31:189–197 (January 15, 2014)

DOI: 10.1089/neu.2013.3069

Investigating the Properties of the Hemodynamic Response Function after Mild Traumatic Brain Injury

Andrew R. Mayer,[1–3] Trent Toulouse,[1] Stefan Klimaj,[1] Josef M. Ling,[1] Amanda Pena,[1] and Patrick S. F. Bellgowan[4,5]

Abstract

Although several functional magnetic resonance imaging (fMRI) studies have been conducted in human models of mild traumatic brain injury (mTBI), to date no studies have explicitly examined how injury may differentially affect both the positive phase of the hemodynamic response function (HRF) as well as the post-stimulus undershoot (PSU). Animal models suggest that the acute and semi-acute stages of mTBI are associated with significant disruptions in metabolism and to the microvasculature, both of which could impact on the HRF. Therefore, fMRI data were collected on a cohort of 30 semi-acute patients with mTBI (16 males; 27.83 ± 9.97 years old; 13.00 ± 2.18 years of education) and 30 carefully matched healthy controls (HC; 16 males; 27.17 ± 10.08 years old; 13.37 ± 2.31 years of education) during a simple sensory-motor task. Patients reported increased cognitive, somatic, and emotional symptoms relative to controls, although no group differences were detected on traditional neuropsychological examination. There were also no differences between patients with mTBI and controls on fMRI data using standard analytic techniques, although mTBI exhibited a greater volume of activation during the task qualitatively. A significant Group × Time interaction was observed in the right supramarginal gyrus, bilateral primary and secondary visual cortex, and the right parahippocampal gyrus. The interaction was the result of an earlier time-to-peak and positive magnitude shift throughout the estimated HRF in patients with mTBI relative to HC. This difference in HRF shape combined with the greater volume of activated tissue may be indicative of a potential compensatory mechanism to injury. The current study demonstrates that direct examination and modeling of HRF characteristics beyond magnitude may provide additional information about underlying neuropathology that is not available with more standard fMRI analyses.

Key words: fMRI; hemodynamic response function; sensorimotor; traumatic brain injury

Introduction

Mild traumatic brain injury (mTBI) remains a poorly understood clinical phenomenon, despite lifetime incidence rates between 110 and 550 per 100,000 persons.[1–3] Recent evidence suggests that the cumulative effects of multiple mTBI may result in a four-fold increase in neurodegenerative diseases[4] and a unique neuropathological syndrome involving tauopathies in periventricular spaces and deep cortical sulci, with an overrepresentation of frontal and medial temporal pathology.[5] A single-episode mTBI is associated with subtle cognitive deficits within the first few weeks of injury that typically resolve spontaneously within 3 to 6 months for approximately 80–95% of patients.[1,3,6] Standard clinical neuroimaging sequences (computed tomography [CT] scans; T1 and T2-weighted images), however, are typically negative for the majority of patients, leading to a proliferation of studies that have attempted to define objective biomarkers of mTBI.[7]

There has been great interest in using functional magnetic resonance imaging (fMRI) to study mTBI given the ability to perform *in vivo* measurements of neuronal function during demanding cognitive tasks[8] as well as during passive mental activity.[9–11] Previous fMRI studies have reported a mixed pattern of both hypo- and hyperactivation during the semi-acute stage of mTBI, as well as no observable group differences.[12–20] During normal neurovascular coupling, the blood oxygen level dependent (BOLD) response represents an amalgamation of signals derived from the ratio of oxy- to deoxyhemoglobin (primary), cerebral blood flow (CBF), and cerebral blood volume (CBV).[21–23] Although the exact nature

[1]The Mind Research Network/Lovelace Biomedical and Environmental Research Institute, Albuquerque, New Mexico.
[2]Neurology Department, University of New Mexico School of Medicine, Albuquerque, New Mexico.
[3]Department of Psychology, University of New Mexico, Albuquerque, New Mexico.
[4]Laureate Institute for Brain Research, Tulsa, Oklahoma.
[5]Faculty of Community Medicine, The University of Tulsa, Tulsa, Oklahoma.

of neurovascular coupling is still being investigated, the BOLD response likely results from the glutamatergic signaling after excitatory neurotransmission and/or underlying increased metabolic demands.[24–26]

The BOLD response is complex in nature, with the canonical hemodynamic response function (HRF) consisting of two primary components—a positive signal change that peaks approximately 4 to 6 sec post-stimulus onset, and a post-stimulus undershoot (PSU) that peaks 6 to 10 sec after the stimulus ends.[21,27] In spite of this complexity, previous research on the BOLD response in both mild and more severe forms of TBI have typically estimated only a single parameter (typically a beta weight) by convolving a canonical HRF (e.g., a gamma variate or a double gamma variate function) with known experimental conditions (e.g., onset of a particular trial) to derive a predictor function (e.g., regressor). Importantly, this assumes that the different aspects of the HRF (positive phase and PSU) and their relationship to each other are largely unaffected by mTBI. To date, only a single study has explicitly examined the HRF in more severe TBI,[28] reporting that although basic visual stimuli were associated with an increased volume of activation in the TBI group, there were no differences in the basic shape of the HRF between groups.

There is a decoupling between CBF and oxidative metabolism after neuronal activation,[29] which leads to an excess in oxygenated blood and a decrease in the ratio of deoxyhemoglobin relative to oxyhemoglobin. This decoupling and subsequent change in the ratio of intravascular oxy- to deoxyhemoglobin primarily drives the positive phase of the BOLD response.[21] The biophysical origins of the PSU remain more controversial. An early model attributed the PSU to temporal delays between when CBF (earlier response) and CBV (delayed response) returned to baseline levels.[21,30] More recent work, however, suggests that the PSU is still present when CBV has returned to baseline,[31] leading others to suggest that increased metabolic demands (cerebral metabolic rate of oxygen [$CMRO_2$]) after cellular signaling may contribute to the PSU.[31,32] Thus, while metabolic changes after injury can be directly assessed using positron emission tomography,[33–35] the BOLD signal may also be affected by metabolic alterations after injury. Finally, other work implicates additional contributing factors to the magnitude of the PSU response such as stimulus properties (duration) and spatial proximity to source of activation.[36,37]

TBI has been shown to reduce cerebral perfusion,[38] decrease vascular reactivity,[39] and decrease the density and diameters of capillaries both at the injury site and diffusely.[40] Metabolic failure after TBI occurs even in the presence of normal perfusion,[41] with an initial decoupling between CBF and the cerebral metabolism rate for glucose (CMR_{glu}) during baseline states, followed by a generally reduced cerebral metabolism.[38,42] Animal models suggest that alterations in CBF and CMR_{glu} may be the most long-lasting physiological deficits of concussion.[42] However, the decoupling between CBF and CMR_{glu} in animal models of mTBI have primarily been observed during baseline states (e.g., anesthetized animals), when a tight coupling[43] exists between CBF, CMR_{glu}, and $CMRO_2$. Thus, there is considerable impetus to more carefully examine the basic properties of the evoked HRF after mTBI.

The current experiment used a simple sensory-motor task with minimal cognitive demands in conjunction with a rapid event-related fMRI paradigm to investigate HRF abnormalities after mTBI. Based on previous results regarding the biomechanical forces accompanying mTBI, we predicted deep subcortical structures such as the thalamus and cerebellum would be more likely to be affected and thus show HRF alterations.[44] We also predicted that trauma-induced changes in microvascular integrity (reduced CBF and reduced microvasculature density) and resulting decreased $CMR_{glu}/CMRO_2$ should result in a reduced magnitude of both the positive (i.e., hypoactivation) and negative (PSU) phases of the BOLD response for patients with mTBI relative to controls.

Methods

Participants

Thirty-two patients with mTBI and 32 sex, age and education-matched controls were recruited for the current study. Two patients were identified as having excessive (greater than three standard deviations [SD]) motion (frame-wise displacement) on two of six parameters[45] and were subsequently eliminated from further analyses along with their matched controls. This left a final dataset of 30 patients with mTBI (14 females, 16 males; 27.83 ± 9.97 years old; 13.00 ± 2.18 years of education) and 30 matched controls (27.17 ± 10.08 years old; 13.37 ± 2.31 years of education). Of note, 24 of the patients with mTBI presented in the current study are independent from our two previous publications examining evoked BOLD responses.[18,46]

Inclusion criteria for the current study were based on the American Congress of Rehabilitation Medicine and included a Glasgow Coma Scale score of 13–15 (at presentation in the emergency department), loss of consciousness (if present) limited to 30 min, and post-traumatic amnesia limited to a 24-h period.[3] All patients with mTBI experienced a closed head injury resulting in an alteration in mental status at minimum (see online Supplementary Table 1 at ftp.liebertpub.com). Eighteen of the 30 patients with mTBI had a CT scan during their emergency department visit, but none of the scans indicated trauma-related pathology. Participants with mTBI and controls were excluded if there was a positive history of neurological disease, psychiatric disturbance, additional closed head injuries with more than 5 min loss of consciousness, learning disorder, attention deficit hyperactivity disorder, or a history of substance or alcohol abuse. At the time of assessment, three of the patients with mTBI were being prescribed medications for trauma-related issues. Informed consent was obtained from subjects according to institutional guidelines at the University of New Mexico.

Clinical assessment

Patients were evaluated both clinically (mean day post-injury = 15.00 ± 4.37) and with brain imaging (mean day post-injury = 14.97 ± 4.88) within 21 days of injury (see online Supplementary Table 1 at ftp.liebertpub.com). To reduce redundancy among similar neuropsychological measures, composite indices were calculated for the cognitive domains of attention, working memory, processing speed, executive function, and memory.[46] Self-report of emotional status (State-Trait Anxiety Index and Beck Depression Inventory-Second Edition), somatic complaints (Neurobehavioral Symptom Inventory), and cognitive complaints (Neurobehavioral Symptom Checklist) were also assessed. When possible, raw test scores were converted to T-scores (mean = 50, SD = 10) using published age-specific norms and then averaged to provide an overall composite score. The Wechsler Test of Adult Reading (WTAR) was also used to provide an estimate of overall premorbid intellectual functioning. The Test of Memory and Malingering (TOMM) allowed assessment of participant effort and cooperation. Independent sample *t* tests or multivariate analyses (MANOVAs) were used to compare demographic and clinical data across patients with mTBI and controls.

Task

All participants completed a sensory-motor detection task while undergoing fMRI on a 3.0 Tesla Siemens Trio scanner. Participants

rested supine in the scanner with their head secured by a forehead strap, with additional foam padding to limit head motion within the head coil. Presentation software (Neurobehavioral Systems) was used for stimulus presentation, synchronization of stimulus events with the MRI scanner, and recording of response times. A white visual fixation cross (visual angle = 0.9 degrees) on a black background was rear-projected using a Sharp XG-C50X LCD projector onto an opaque white Plexiglas projection screen. Auditory stimuli were presented with an Avotec Silent Scan 3100 Series System.

Participants were simultaneously presented with a visual (blue box; visual angle = 4.3 × 6.5 degrees) and auditory (2000 Hz resampled with a 10 ms linear ramp) stimulus of 300 ms duration across 35 different trials. Participants were asked to press a button with their right index finger on the presentation of multisensory stimuli. The duration of the intertrial interval varied from 4 to 8 sec to prevent the development of temporal expectations, non-linear summing of the hemodynamic response,[47] and to allow for the best sampling of the hemodynamic response.[48] All participants briefly practiced the task in a separate session before scanning to ensure that they understood directions (≈ 99% task accuracy across both groups).

MRI

High resolution 5-echo multi-echo MPRAGE T1 (TR [repetition time] = 2.53 sec, 7 degree flip angle, TE [echo times] = 1.64, 3.5, 5.36, 7.22, 9.08 ms, number of excitations [NEX] = 1, slice thickness = 1 mm, FOV [field of view] = 256 mm, resolution = 256 × 256) and T2 [TE = 77.0 ms, TR = 1.55 sec, flip angle 152 degrees, NEX = 1, slice thickness = 1.5 mm, FOV = 220 mm, matrix = 192 × 192, voxel size = 1.15 × 1.15 × 1.5 mm^3) sequences were collected on a 3 Tesla Siemens Trio scanner. Susceptibility weighted imaging (TR = 28 ms; TE = 20 ms; flip angle 15 degrees; bandwidth = 120 Hz/Px; FOV = 180 × 240 mm; matrix = 177 × 256; slice thickness = 1.5 mm; number of slices per slab = 88) were collected on a smaller cohort of patients (N = 22) to better characterize petechial hemorrhages.

Echo-planar images (EPI) were collected using a single-shot, gradient-echo echoplanar pulse sequence (TR = 2000 ms; TE = 29 ms; flip angle = 75 degrees; FOV = 240 mm; matrix size = 64 × 64). Thirty-three contiguous sagittal 3.5-mm thick slices with a gap factor of 1.05 mm were selected to provide whole-brain coverage (voxel size: 3.75 × 3.75 × 4.55 mm). The first three images of the run were eliminated to account for T1 equilibrium effects, resulting in a total of 114 images for the final analyses.

Image processing and statistical analyses

Functional images were generated using Analysis of Functional NeuroImages software package.[49] Time series images were spatially registered in both two- and three-dimensional space to the second EPI image of the first run to minimize effects of head motion, temporally interpolated to correct for slice-time acquisition differences, de-spiked and blurred with a 6 mm full width at half maximum (FWHM) Gaussian kernel. Anatomical and functional images were then interpolated to volumes with 3 mm^3 voxels and converted to a standard stereotaxic coordinate space.[50] A deconvolution analysis was then performed on a voxel-wise basis to generate an unbiased HRF for the multisensory-motor stimuli. In addition, participants' six motion parameters were entered as regressors of no interest in the deconvolution analyses to reduce the impact of head motion on patterns of functional activation. Each HRF was derived relative to the baseline state (visual fixation plus baseline gradient noise) and based on the first 20 sec (10 images) post-stimulus onset.

The general form of a single condition deconvolution analysis (http://afni.nimh.nih.gov/afni/doc/manual/3dDeconvolve) based on 10 parameters can be represented by the following equation:

$$\begin{aligned} Y(n) &= \beta_0 + \beta_1 n + h(0)f(n) + h(1)f(n-1) \\ &\quad + \cdots + h(9)f(n-9) + e(n) \\ &= \beta_0 + \beta_1 n + \sum_{i=0}^{9} h(i)f(n-i) + e(n) \end{aligned} \quad \text{(Eq.1)}$$

where the observed signal (Y) at each time point (n) is defined as a linear combination of a constant term (β_0), linear (β_1) or higher-order polynomial term, and the experimental condition (denoted by the vector h) multiplied by a binary vector (f) indicating whether the experimental condition occurred on the current and/or previous nine images. The solution is optimized by minimizing the ordinary sum of squares of the residual error term, represented by $e(n)$. Resulting beta coefficients were then normalized by dividing by the average model intercept (β_0) across the experimental run to form an estimate of percent signal change (PSC).

A one-way analysis of covariance (ANCOVA) with group as the factor was first used to compare the peak of the HRF (images occurring four to eight sec post-cue onset) as part of a more standard analytic approach. Within-group comparisons were also performed to identify the neuronal networks activated by the task.

A 2 × 8 (Group × Time) voxel-wise repeated-measures mixed-effect ANCOVA was then conducted to examine how mTBI affects different components of the HRF. An $AR(1)$ autoregressive model was used to model the dependence of the time series data for the covariance matrix,[51] and subjects were treated as a random effect. In this analytic framework, a Group × Time interaction indicates regions where the HRF differed as a function of time. The main effect of time represents regions exhibiting variability across different coefficients and was deemed to be of insufficient interest (i.e., a high-rate of significant effects secondary to variability) for follow-up.

To further qualify group differences in the HRF for significant regions of interest (ROI), differences in peak, time-to-peak, area under the curve (AUC) and the FWHM were calculated using a non-linear regression with a double gamma variate function defined by:

$$M(t) = A_0(t-T_0)^{E_0} \times e^{-(t-T_0)/D_0} - A_1(t-T_1)^{E_1} \times e^{-(t-T_1)/D_1} \quad \text{(Eq.2)}$$

where t is the current time point and A_0, T_0, E_0, D_0 correspond to the peak amplitude, time delay, rise rate, and decay rate for the positive HRF response, and A_1, T_1, E_1, D_1 correspond to the same parameters for the PSU. A significant drawback of this approach, however, is the modelling of 8 parameters (double gamma variate function) for the 10 coefficients estimated from the deconvolution, significantly increasing the likelihood of data overfitting. To partially reduce this limitation, parameters were only fit for group-averaged HRF data followed by estimation of peak and peak latency using the Matlab Symbolic Equation package. The FWHM and the absolute value of the AUC were calculated for both the positive HRF response and the PSU.

For all analyses, a significance threshold corresponding to $p < 0.005$ was applied in combination with a minimum cluster size threshold of 1472 microliters (23 native voxels) to minimize false positives. This resulted in a corrected p value of 0.05 based on 10,000 Monte Carlo simulations.[52]

Results

Neuropsychological and clinical measures

Independent samples t tests indicated that there were no significant differences between patients with mTBI and HC ($p > 0.10$) on

major demographic variables (age, education, or sex) or for hand preference as assessed by the Edinburgh Handedness Inventory.[53]

A compilation of all major neuropsychological and clinical indices are presented in Table 1. One HC was not able to complete the neuropsychological testing battery, and another HC was an outlier on the TOMM in spite of normal performance on all other metrics. Therefore, this subject's data were removed for the TOMM. Independent samples *t* tests indicated a significant difference for the emotionality index ($t_{1,58} = 2.75$, $p < 0.05$; mTBI > HC), with controls exhibiting below normal (composite T = 43.03) levels of depression and anxiety. There was also a significant difference ($t_{1,57} = -2.36$, $p < 0.05$; HC > mTBI) in estimated levels of premorbid intellectual functioning (WTAR) in spite of similar educational backgrounds. Finally, there was a non-significant trend for difference in levels of effort (TOMM) between the two groups ($t_{1,32.10} = -1.81$, $p = 0.08$; mTBI > HC), although effort for both groups was in the normal range (T ≥ 50).

The composite indices of attention, working memory, memory, processing speed, and executive functioning were correlated to varying degrees (*r*'s ranged from −0.08 to 0.71). Therefore, a MANCOVA was performed to examine group differences in the cognitive scores using WTAR as an additional covariate. The multivariate effect of group was not significant ($p > 0.10$), although the univariate effect for processing speed was significant ($F_{1,56} = 4.00$, $p = 0.05$), with group means indicating slowed processing speed in the mTBI group.

A MANOVA was also performed on the three different indices obtained from the Neurobehavioral Symptom Inventory. The multivariate effect of group was significant ($F_{3,56} = 6.39$, $p = 0.001$), with follow-up univariate tests indicating that patients with mTBI reported more cognitive ($F_{1,58} = 9.86$, $p < 0.005$), emotional ($F_{1,58} = 18.87$, $p < 0.005$) and somatic ($F_{1,58} = 16.86$, $p < 0.005$) complaints than controls.

Table 1. Neuropsychological and Clinical Summary Measures

	mTBI	*HC*	*Effect sizes*
Demographic	Mean (SD)	Mean (SD)	
Sex	16 M	16 M	N/A
Age	27.83 (9.97)	27.17 (10.08)	0.07
Education	13.00 (2.18)	13.37 (2.31)	−0.16
HQ	82.47 (38.60)	86.92 (33.59)	−0.12
Neuropsych			
Attention[a]	52.37 (4.43)	53.44 (6.01)	−0.20
Memory[a]	51.67 (6.93)	51.96 (7.00)	−0.04
WM[a]	51.45 (6.39)	51.99 (5.43)	−0.09
PS[a]	43.25 (5.36)	46.67 (6.97)	−0.55
EF[a]	49.70 (6.12)	49.57 (4.55)	0.02
WTAR	50.00 (8.81)	55.07 (7.64)	−0.62
TOMM	54.87 (4.02)	50.36 (12.62)	0.54
Self-report			
Emotional	48.53 (8.83)	43.03 (6.49)	0.72
NBSI-Som	7.83 (6.90)	2.07 (3.40)	1.12
NBSI-Cog	4.23 (3.58)	1.77 (2.39)	0.82
Days Post-injury			
Imaging	14.97 (4.88)	N/A	
Neuropsych	15.00 (4.37)	N/A	

mTBI, mild traumatic brain injury; HC, healthy control; SD = standard deviation; HQ, handedness quotient; WM, working memory; PS, processing speed; EF, executive function; WTAR, Wechsler Test of Adult Reading; TOMM, Test of Memory Malingering; NBSI-Som, Neurobehavioral Symptom Inventory somatic complaints (Cog, cognitive complaints); N/A, not applicable.

[a]Means, standard deviations, and effect sizes for neuropsychological indices reported after correction for WTAR as covariate.

Behavioral data

There were no outliers on measures of accuracy or response time for either group. Accuracy was near ceiling for both mTBI (99.7 ± 1.1%) and HC (99.4 ± 1.1%) samples such that additional analyses were not conducted. An ANCOVA with WTAR as a covariate was performed to examine group differences in median response times during task performance, but no significant differences in group performance were observed ($p > 0.10$).

Structural imaging data

T1, T2, and susceptibility-weighted (when available) MRI images were reviewed by a neuroradiologist blinded to patient diagnosis. Three of the 30 patients with mTBI (all with negative CT scan) were deemed to have MRI findings that may have been secondary to trauma. Specific MRI findings included a subtle T1 hypointensity in the paracentral upper pons, clusters of potential Virchow-Robin spaces in the parietal white matter, and fluid signal in the left temporal lobe possibly related to volume loss. In contrast, none of the HC had any trauma-related positive findings on neuroradiological reads.

Functional imaging data

Two MANOVAs were first conducted to investigate any potential group differences in head motion (both rotational and translational displacements in image space), which could confound our interpretation of fMRI data. Results indicated that the multivariate effect of group, however, was not significant for translational motion ($p > 0.10$) and only a trend for rotational motion ($p = 0.09$), with effect sizes (Cohen *d*) for the six parameters ranging from −0.05 to 0.61.

Standard analyses of HRF peak images

A voxel-wise ANCOVA with group as a factor and pre-morbid intelligence quotient as a covariate was first performed to compare the images (4 to 8 sec post-stimulus onset) corresponding to the peak of the hemodynamic response function (i.e., more standard analyses). Results did not indicate any significant group differences in whole-brain analyses after correction for multiple comparisons.

Peak images were also examined for within-group effects (Fig. 1) to determine the regions responding to the task. Regions of significant activation were determined by comparing PSC of each group to baseline. Regions demonstrating activation across both the HC and mTBI groups included the bilateral primary and secondary auditory cortex (Brodmann areas [BA] 13/22/40/41/42), bilateral primary and secondary visual cortex (BA 17/18/19/30), bilateral cerebellum extending into fusiform and parahippocampal gyri (BA 19/35/36/37), left sensori-motor cortex (BA 2/3/4/6/40), left thalamic/subcortical (mammillary body and substantia nigra) nuclei and bilateral cuneus extending into the posterior cingulate gyrus (BA 17/18/23/30/31). Although the overall volume of activation could not be statistically evaluated across the two groups, the volume of activation was larger for the mTBI group (309.90 mL) relative to the HC (138.62 mL), with increased regions of activation occurring within the primary and secondary visual cortex, auditory cortex and the cerebellum.

A 2 × 8 (Group × Time) (2 to 18 sec post-stimulus onset) mixed effects whole-brain ANCOVA was performed next to examine

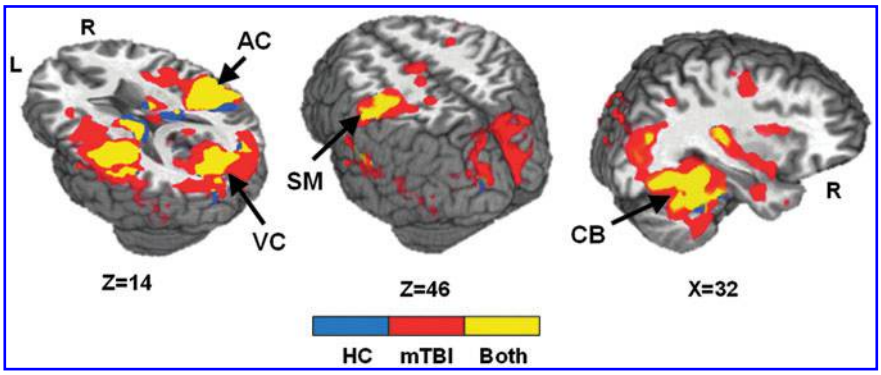

FIG. 1. This figure presents the within-group comparisons of the peak activation (4 to 8 sec post-stimulus onset) percent signal change data. Voxels that exhibited unique activation for healthy controls (HC) are presented in blue and for patients with mild traumatic brain injury (mTBI) in red. Voxels with yellow coloring were commonly activated across both groups. Qualitatively, mTBI demonstrated a greater volume of activation in the primary/secondary visual (VC) and auditory (AC) cortex, sensorimotor cortex (SM) and the cerebellum (CB). Slice locations are provided according to the Talairach atlas.

group differences in the shape of the HRF. The main effect of group was not significant after correction for false positives. However, there were several regions (Fig. 2) that demonstrated a significant Group × Time interaction including the right supramarginal gyrus (BA 40), bilateral primary (BA 17) and secondary (BA 18/19) visual cortex, and the right parahippocampal gyrus (BA 30/35/36/37). Follow-up simple effects tests were then conducted at each time point within each of these regions to examine for group differences. Results indicated that mTBI showed significantly increased activation at the first time point (2 sec post-stimulus onset) for all ROI with the exception of the right supramarginal gyrus. In contrast, mTBI showed significantly decreased activation in the

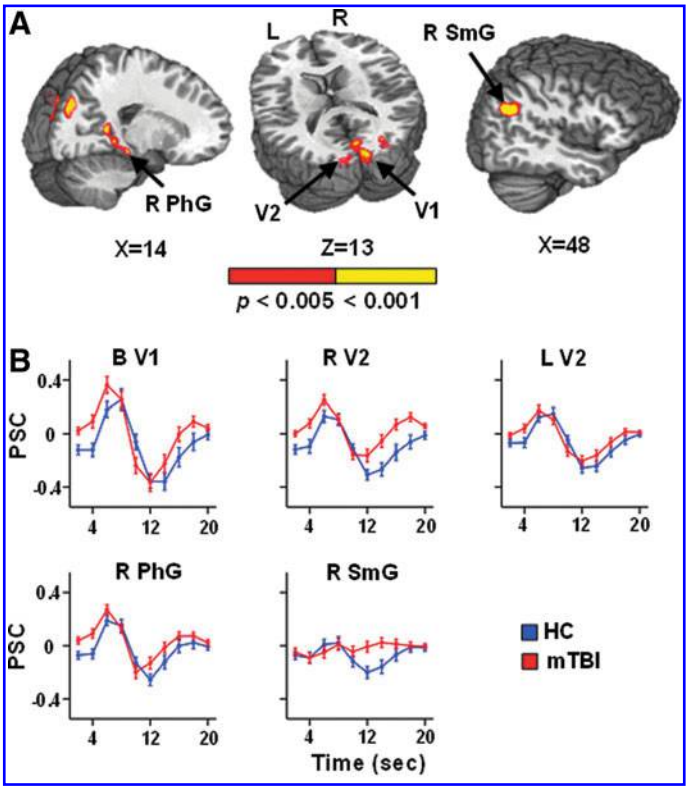

FIG. 2. Panel **A** presents the regions that exhibited a significant Group × Time interaction. These regions included the right supramarginal gyrus (R SmG), bilateral primary visual cortex (B V1), secondary right (R V2) and left (L V2) visual cortex, and the right parahippocampal gyrus (R PhG). The mean hemodynamic response function of each region of interest (ROI) for healthy controls (HC; blue line) and patients with mild traumatic brain injury (mTBI; red line) are presented in Panel **B**, with error bars reflecting the standard error of the mean. Simple effects testing indicated that mTBI had significantly increased activation 2 sec post-stimulus onset for all ROIs with the exception of the right supramarginal gyrus. Significantly decreased magnitude of the post-stimulus undershoot for patients with mTBI was observed in the bilateral primary visual cortex (10 sec, 16 sec, 18 sec), right secondary visual cortex (12 sec, 14 sec, 16 sec, 18 sec) and supramarginal gyrus (12 sec, 14 sec). Slice locations are provided according to the Talairach atlas.

primary visual cortex (10 sec, 16 sec, 18 sec), right secondary visual cortex (12 sec, 14 sec, 16 sec, 18 sec), and supramarginal gyrus (12 sec, 14 sec) during the PSU. Similar non-significant trends in the PSU were also observed in the right parahippocampal gyrus.

To further qualify the above findings, the group-averaged HRF from each region was then fit with a double gamma variate function. A single value was then calculated from the fitted function for each group, precluding statistical analysis. A qualitative comparison of the magnitude of the fitted values (Table 2), however, indicated that patients with mTBI exhibited larger peak amplitude, AUC, and FWHM during the positive phase of the HRF response within all ROI, with the largest effects observed within the primary visual cortex, right parahippocampal gyrus, and right supramarginal gyrus. During the PSU, mTBI showed a decreased response for these same parameters (peak amplitude, AUC, and FWHM) within every ROI except the primary visual cortex. Finally, the time-to-peak for both the positive and negative (i.e., PSU) phases of the HRF occurred earlier for patients with mTBI for all ROIs.

Discussion

The HRF represents a complicated physiological response that is dependent on changes in blood flow, blood volume, and ratio of deoxyhemoglobin to oxyhemoglobin, representing an indirect measure of neuronal activity.[54] It is widely recognized that the HRF comprises two major components consisting of both a positive and a negative phase (PSU), although previous fMRI studies of mTBI research have typically focused only on a single summary statistic. Current results did not indicate any significant group differences during the positive phase of the HRF using more traditional analytic techniques during a simple sensorimotor task. In contrast, significant effects were observed in the bilateral visual cortex, right supramarginal gyrus, and right parahippocampal cortex when the entire HRF was examined. Follow-up testing suggested that these effects were primarily driven by patients with mTBI exhibiting both a faster initial increase in the hemodynamic response (significant difference at the 2 sec time point) as well as reduction in the magnitude of the PSU relative to the HC group (across time points 10–18 sec).

Although patients with mTBI self-reported increased neurobehavioral symptoms (i.e., cognitive, emotional, and somatic symptoms) during the semi-acute injury phase, there were no statistically significant group differences on neuropsychological testing. This finding is consistent with previous results from our group in a largely independent cohort,[46] with null findings on traditional neuropsychological testing occurring potentially as a result of several different factors. First, previous data have indicated that cognitive deficits and other neurobehavioral sequelae may resolve within the first week of injury,[55] whereas our clinical data were collected approximately 2 weeks post-injury. Second, the effect sizes for neuropsychological tests are traditionally reported to be in the small to medium range during the semi-acute phase of injury.[56] Current effect sizes were generally in this range (Table 1), and even assuming a medium effect size (Cohen $d = 0.50$), the current sample was only powered at 0.48 for detecting these subtle neuropsychological deficits with the current sample size. Finally, it is possible that individual patients experience different objective symptoms (e.g., patient A has processing speed deficits whereas patient B has executive dysfunction), and this heterogeneity in functioning across individual cognitive domains may be obscured during more traditional analyses that compare group means.[57]

We had predicted that the diencephalon, deep cortical structures, and cerebellum would likely show the greatest abnormalities in the HRF based on our previous results from independent cohorts[20,46] and biomechanical models of injury.[44] Current results, however, indicated an increased hemodynamic response in the bilateral primary/secondary visual cortex and the right parahippocampal gyrus approximately 2 to 4 sec post-stimulus onset. Quantitative modeling of the group-differences in the HRF suggested that these findings were likely the result of a faster time-to-peak within these regions for patients with mTBI relative to controls. In addition, visual inspection and volume counts of the within subject activation maps (Fig. 1) indicated larger areas of activation for the patients with mTBI relative to controls. Increased volume of activation and more rapid time-to-peak suggests that these regions are being recruited earlier and to a greater extent in patients with mTBI, indicating a potential compensatory measure after injury. Previous fMRI studies, however, have reported increased activation in

Table 2. Modeled Parameters of the Hemodynamic Response Function

	Peak		*TTP*		*FWHM*		*AUC*	
Positive phase	*HC*	*TBI*	*HC*	*TBI*	*HC*	*TBI*	*HC*	*TBI*
L V2	0.181	0.191	2.638	2.308	1.559	1.693	0.269	0.310
R PhG	0.227	0.292	2.489	2.277	1.550	1.704	0.336	0.482
SmG	0.054	0.179	2.484	2.266	0.797	0.571	0.040	0.102
R V2	0.236	0.255	2.415	2.227	1.054	1.766	0.237	0.428
V1	0.289	0.397	2.672	2.387	1.529	1.837	0.411	0.689
	Peak		*TTP*		*FWHM*		*AUC*	
PSU	*HC*	*TBI*	*HC*	*TBI*	*HC*	*TBI*	*HC*	*TBI*
L V2	−0.257	−0.211	5.429	4.927	2.887	2.610	0.738	0.546
R PhG	−0.237	−0.208	4.777	4.273	2.178	1.646	0.514	0.333
SmG	−0.173	−0.037	4.931	3.716	3.420	1.566	0.603	0.064
R V2	−0.280	−0.198	5.221	4.487	3.261	1.851	0.906	0.354
V1	−0.379	−0.382	5.431	4.766	2.754	2.158	1.040	0.811

TTP, time-to-peak; FWHM, full width half-maximum; AUC, area under the curve; HC, health control; mTBI, mild traumatic brain injury; L, left; R, right; V2, secondary visual cortex; PhG, parahippocampal gyrus; SmG, supramarginal gyrus; V1, primary visual cortex; PSU, post-stimulus undershoot.

mild[16] and more severe[28] TBI as well as a reduced volume of activation,[58] including our previous work.[46] Thus, more studies are needed to examine whether these conflicting findings are secondary to differences in task difficulty or other clinical factors.

In addition, the bilateral primary/secondary visual cortex, right hippocampus, and right supramarginal gyrus also showed a reduced PSU relative to HC. As discussed in the Introduction, the relative contributions from vasculature and/or metabolic mechanisms to the PSU is heavily debated,[36] indicating that the potential impacts of injury on physiology are even more confounding. The PSU is dependent on both oxidative metabolism and delayed CBV recovery[37,59] and may be biased toward arteriolar-dependent changes in oxyhemoglobin levels.[60] An alteration in the normal relationship between CBF and CBV after TBI could result in a decrease in the amplitude of the PSU.[21] Reductions in CBF as a function of age, however, have not directly translated into a reduction in the BOLD PSU,[61] suggesting that other mechanisms such as a decrease in the number/width of microvessels[40] and/or alterations in vasocompliance after injury may also be contributing factors. Moreover, the exact spatial locations of the reductions in CBF are likely to be dependent on initial biomechanical injury forces, which are variable across individual patients.

Similarly, it has also been suggested that cellular signaling and the resultant increase in $CMRO_2$ may be a critical driver of the PSU.[31,32] A close coupling exists between CBF, $CMRO_2$, and CMR_{glu} during baseline metabolism, with a decoupling between CBF/CMR_{glu} and $CMRO_2$ after neuronal activity.[29,62] This uncoupling may occur because glucose is consumed through anaerobic glycolysis rather than oxidative metabolism immediately after neuronal activity. Previous results from the animal literature indicate a complex response in CMR_{glu} after mTBI that is characterized by an initial increase (lasting for approximately 20 min) followed by a reduction that lasts for several days post-injury.[42] Therefore, the reduced PSU observed in the current experiment may also result from a reduced baseline availability of CMR_{glu}, given the known relationship $CMRO_2$ and CMR_{glu}.[63]

Finally, it is important to note that the current positive findings were relatively limited in scope to regions within the visual cortex and medial temporal cortex. Specifically, several other regions implicated in the task during within-subject analyses (e.g., auditory cortex, motor cortex, supplementary motor area, cerebellum, and subcortical regions) did not exhibit any group differences across the multiple time points constituting the HRF. The null findings in these regions are similar to a previous study that explicitly modeled the HRF in patients with severe TBI with a gamma variate function.[28] Although extending the results from simple sensory tasks to more complex cognitive processes is challenging, these largely null findings do not directly contradict the large body of literature on evoked BOLD responses in mTBI. In addition, the HRF in all areas exhibiting the interaction effect was characterized by a downward shift for HC relative to the mTBI group. Therefore, while all data were empirically evaluated and corrected for false positives, it will be important to replicate current findings in an independent sample of patients with mTBI.

There are several limitations to the current study. First, as reviewed in the introduction, animal studies have indicated impaired neuronal function, impaired neural control of the microvasculature, direct damage to the microvascular system, metabolic disruptions, and/or a combination of these findings following the transmission of biomechanical forces to the parenchyma.[40,64] Thus, there are several underlying pathophysiological mechanisms that could putatively impact on the measurement of the HRF, and the contribution of each is difficult to disambiguate on the macroscopic level that neuroimaging data are obtained. Second, a small percentage of subjects were also being administered different medications for trauma-related symptoms that could have affected neurovascular coupling and hence the underlying HRF.

Finally, modeling three (i.e., a single gamma variate function) or eight free parameters (i.e., a double gamma variate function) based on 10 data points (i.e., measured HRF) increases the likelihood of modeling many different signal types (i.e., noise) rather than a true HRF. Further, the hemodynamic signal has a relatively low signal-to-noise ratio on a voxel-wise basis, which precluded fitting the HRF on an individual subject level. Previous studies[28,65] have partially overcome this limitation by fitting the HRF with a gamma variate function, and upsampling the temporal resolution of the data. A single gamma variate function, however, precludes the examination of the PSU,[28] which was a primary objective of the current study.

Conclusion

Detectable functional imaging differences in patients with mTBI have been elusive. Both venous[30] and arteriolar compliance[66] models of the BOLD signal are heavily dependent on CBF and CBV, and therefore on the integrity of both venal and arteriole vessel reactivity. The vasculature and metabolic changes associated with TBI could significantly alter either the positive or the negative phase of the BOLD signal, and analysis relying on convolution of a canonical HRF with the observed signal may mask these different effects. By modeling the full time course of a deconvolved HRF, the current analysis provides a more comprehensive approach for investigating neuronal pathology after mTBI.

Author Disclosure Statement

No competing financial interests exist.

References

1. Belanger, H.G., Vanderploeg, R.D., Curtiss, G., and Warden, D.L. (2007). Recent neuroimaging techniques in mild traumatic brain injury. J. Neuropsychiatry Clin. Neurosci. 19**,** 5–20.
2. Faul, M., Xu, L., Wald, M.M., and Coronado, V.G. (2010).*Traumatic brain injury in the United States: emergency department visits, hospitalizations, and deaths 2002–2006.* Centers for Disease Control and Prevention: Atlanta.
3. Bigler, E.D. (2008). Neuropsychology and clinical neuroscience of persistent post-concussive syndrome. J. Int. Neuropsychol. Soc. 14**,** 1–22.
4. Lehman, E.J., Hein, M.J., Baron, S.L., and Gersic, C.M. (2012). Neurodegenerative causes of death among retired National Football League players. Neurology 79**,** 1970–1974.
5. McKee, A.C., Stein, T.D., Nowinski, C.J., Stern, R.A., Daneshvar, D.H., Alvarez, V.E., Lee, H.S., Hall, G., Wojtowicz, S.M., Baugh, C.M., Riley, D.O., Kubilus, C.A., Cormier, K.A., Jacobs, M.A., Martin, B.R., Abraham, C.R., Ikezu, T., Reichard, R.R., Wolozin, B.L., Budson, A.E., Goldstein, L.E., Kowall, N.W., and Cantu, R.C. (2013). The spectrum of disease in chronic traumatic encephalopathy. Brain 136**,** 43–64.
6. Iverson, G.L. (2005). Outcome from mild traumatic brain injury. Curr. Opin. Psychiatry 18**,** 301–317.
7. Bigler, E.D. and Maxwell, W.L. (2012). Neuropathology of mild traumatic brain injury: relationship to neuroimaging findings. Brain Imaging Behav. 6**,** 108–136.
8. McDonald, B.C., Saykin, A.J., and McAllister, T.W. (2012). Functional MRI of mild traumatic brain injury (mTBI): progress and perspectives from the first decade of studies. Brain Imaging Behav. 6**,** 193–207.
9. Johnson, B., Zhang, K., Gay, M., Horovitz, S., Hallett, M., Sebastianelli, W., and Slobounov, S. (2012). Alteration of brain default network in subacute phase of injury in concussed individuals: resting-state fMRI study. Neuroimage 59**,** 511–518.

10. Mayer, A.R., Mannell, M.V., Ling, J., Gasparovic, C., and Yeo, R.A. (2011). Functional connectivity in mild traumatic brain injury. Hum. Brain Mapp. 32, 1825–1835.
11. Shumskaya, E., Andriessen, T.M., Norris, D.G., and Vos, P.E. (2012). Abnormal whole-brain functional networks in homogeneous acute mild traumatic brain injury. Neurology 79, 175–182.
12. Lovell, M.R., Pardini, J.E., Welling, J., Collins, M.W., Bakal, J., Lazar, N., Roush, R., Eddy, W.F., and Becker, J.T. (2007). Functional brain abnormalities are related to clinical recovery and time to return-to-play in athletes. Neurosurgery 61, 352–360.
13. Jantzen, K.J., Anderson, B., Steinberg, F.L., and Kelso, J.A. (2004). A prospective functional MR imaging study of mild traumatic brain injury in college football players. AJNR Am. J. Neuroradiol. 25, 738–745.
14. McAllister, T.W., Saykin, A.J., Flashman, L.A., Sparling, M.B., Johnson, S.C., Guerin, S.J., Mamourian, A.C., Weaver, J.B., and Yanofsky, N. (1999). Brain activation during working memory 1 month after mild traumatic brain injury: a functional MRI study. Neurology 53, 1300–1308.
15. McAllister, T.W., Sparling, M.B., Flashman, L.A., Guerin, S.J., Mamourian, A.C., and Saykin, A.J. (2001). Differential working memory load effects after mild traumatic brain injury. Neuroimage 14, 1004–1012.
16. Slobounov, S.M., Zhang, K., Pennell, D., Ray, W., Johnson, B., and Sebastianelli, W. (2010). Functional abnormalities in normally appearing athletes following mild traumatic brain injury: a functional MRI study. Exp. Brain Res. 202, 341–354.
17. Smits, M., Dippel, D.W., Houston, G.C., Wielopolski, P.A., Koudstaal, P.J., Hunink, M.G., and van der Lugt, A. (2009). Post-concussion syndrome after minor head injury: brain activation of working memory and attention. Hum. Brain Mapp. 30, 2789–2803.
18. Mayer, A.R., Yang, Z., Yeo, R.A., Pena, A., Ling, J.M., Mannell, M.V., Stippler, M., and Mojtahed, K. (2012). A functional MRI study of multimodal selective attention following mild traumatic brain injury. Brain Imaging Behav. 6, 343–354.
19. Witt, S.T., Lovejoy, D.W., Pearlson, G.D., and Stevens, M.C. (2010). Decreased prefrontal cortex activity in mild traumatic brain injury during performance of an auditory oddball task. Brain Imaging Behav. 4, 232–247.
20. Yang, Z., Yeo, R.A., Pena, A., Ling, J.M., Klimaj, S., Campbell, R., Doezema, D., and Mayer, A.R. (2012). An fMRI study of auditory orienting and inhibition of return in pediatric mild traumatic brain injury. J. Neurotrauma 29, 2124–2136.
21. Buxton, R.B., Uludag, K., Dubowitz, D.J., and Liu, T.T. (2004). Modeling the hemodynamic response to brain activation. Neuroimage 23, Suppl 1, S220–S233.
22. Logothetis, N.K. (2008). What we can do and what we cannot do with fMRI. Nature 453, 869–878.
23. Shen, Q., Ren, H., and Duong, T.Q. (2008). CBF, BOLD, CBV, and CMRO(2) fMRI signal temporal dynamics at 500-msec resolution. J. Magn Reson. Imaging 27, 599–606.
24. Attwell, D., Buchan, A.M., Charpak, S., Lauritzen, M., Macvicar, B.A., and Newman, E.A. (2010). Glial and neuronal control of brain blood flow. Nature 468, 232–243.
25. Logothetis, N.K. and Wandell, B.A. (2004). Interpreting the BOLD signal. Annu. Rev. Physiol. 66, 735–769.
26. Mangia, S., Tkac, I., Gruetter, R., Van de Moortele, P.F., Maraviglia, B., and Ugurbil, K. (2007). Sustained neuronal activation raises oxidative metabolism to a new steady-state level: evidence from 1H NMR spectroscopy in the human visual cortex. J. Cereb. Blood Flow Metab. 27, 1055–1063.
27. Cohen, M.S. (1997). Parametric analysis of fMRI data using linear systems methods. Neuroimage 6, 93–103.
28. Palmer, H.S., Garzon, B., Xu, J., Berntsen, E.M., Skandsen, T., and Haberg, A.K. (2010). Reduced fractional anisotropy does not change the shape of the hemodynamic response in survivors of severe traumatic brain injury. J. Neurotrauma 27, 853–862.
29. Fox, P.T. and Raichle, M.E. (1986). Focal physiological uncoupling of cerebral blood flow and oxidative metabolism during somatosensory stimulation in human subjects. Proc. Natl. Acad. Sci. U. S. A 83, 1140–1144.
30. Buxton, R.B., Wong, E.C., and Frank, L.R. (1998). Dynamics of blood flow and oxygenation changes during brain activation: the balloon model. Magn. Reson. Med. 39, 855–864.
31. Lu, H., Golay, X., Pekar, J.J., and Van Zijl, P.C. (2004). Sustained poststimulus elevation in cerebral oxygen utilization after vascular recovery. J. Cereb. Blood Flow Metab. 24, 764–770.
32. Schroeter, M.L., Kupka, T., Mildner, T., Uludag, K., and von Cramon, D.Y. (2006). Investigating the post-stimulus undershoot of the BOLD signal—a simultaneous fMRI and fNIRS study. Neuroimage 30, 349–358.
33. Gross, H., Kling, A., Henry, G., Herndon, C., and Lavretsky, H. (1996). Local cerebral glucose metabolism in patients with long-term behavioral and cognitive deficits following mild traumatic brain injury. J. Neuropsychiatry Clin. Neurosci. 8, 324–334.
34. Peskind, E.R., Petrie, E.C., Cross, D.J., Pagulayan, K., McCraw, K., Hoff, D., Hart, K., Yu, C.E., Raskind, M.A., Cook, D.G., and Minoshima, S. (2011). Cerebrocerebellar hypometabolism associated with repetitive blast exposure mild traumatic brain injury in 12 Iraq war Veterans with persistent post-concussive symptoms. Neuroimage 54, Suppl 1, S76–S82.
35. Prins, M.L., Alexander, D., Giza, C.C., and Hovda, D.A. (2013). Repeated mild traumatic brain injury: mechanisms of cerebral vulnerability. J. Neurotrauma 30, 30–38.
36. Harshbarger, T.B. and Song, A.W. (2008). Differentiating sensitivity of post-stimulus undershoot under diffusion weighting: implication of vascular and neuronal hierarchy. PLoS. ONE. 3, e2914.
37. van Zijl, P.C., Hua, J., and Lu, H. (2012). The BOLD post-stimulus undershoot, one of the most debated issues in fMRI. Neuroimage 62, 1092–1102.
38. Soustiel, J.F. and Sviri, G.E. (2007). Monitoring of cerebral metabolism: non-ischemic impairment of oxidative metabolism following severe traumatic brain injury. Neurol. Res. 29, 654–660.
39. Bouma, G.J. and Muizelaar, J.P. (1992). Cerebral blood flow, cerebral blood volume, and cerebrovascular reactivity after severe head injury. J. Neurotrauma 9, Suppl 1, S333–S348.
40. Park, E., Bell, J.D., Siddiq, I.P., and Baker, A.J. (2009). An analysis of regional microvascular loss and recovery following two grades of fluid percussion trauma: a role for hypoxia-inducible factors in traumatic brain injury. J. Cereb. Blood Flow Metab. 29, 575–584.
41. Vespa, P.M., O'Phelan, K., McArthur, D., Miller, C., Eliseo, M., Hirt, D., Glenn, T., and Hovda, D.A. (2007). Pericontusional brain tissue exhibits persistent elevation of lactate/pyruvate ratio independent of cerebral perfusion pressure. Crit. Care Med. 35, 1153–1160.
42. Giza, C.C. and Hovda, D.A. (2001). The Neurometabolic Cascade of Concussion. J. Athl. Train. 36, 228–235.
43. Sokoloff, L., Reivich, M., Kennedy, C., Des Rosiers, M.H., Patlak, C.S., Pettigrew, K.D., Sakurada, O., and Shinohara, M. (1977). The [14C]deoxyglucose method for the measurement of local cerebral glucose utilization: theory, procedure, and normal values in the conscious and anesthetized albino rat. J. Neurochem. 28, 897–916.
44. Zhang, L., Yang, K.H., and King, A.I. (2004). A proposed injury threshold for mild traumatic brain injury. J. Biomech. Eng 126, 226–236.
45. Mayer, A.R., Franco, A.R., Ling, J., and Canive, J.M. (2007). Assessment and quantification of head motion in neuropsychiatric functional imaging research as applied to schizophrenia. J. Int. Neuropsychol. Soc. 13, 839–845.
46. Mayer, A.R., Mannell, M.V., Ling, J., Elgie, R., Gasparovic, C., Phillips, J.P., Doezema, D., and Yeo, R.A. (2009). Auditory orienting and inhibition of return in mild traumatic brain injury: A FMRI study. Hum. Brain Mapp. 30, 4152–4166.
47. Glover, G.H. (1999). Deconvolution of impulse response in event-related BOLD fMRI. Neuroimage 9, 416–429.
48. Burock, M.A., Buckner, R.L., Woldorff, M.G., Rosen, B.R., and Dale, A.M. (1998). Randomized event-related experimental designs allow for extremely rapid presentation rates using functional MRI. Neuroreport 9, 3735–3739.
49. Cox, R.W. (1996). AFNI: Software for analysis and visualization of functional magnetic resonance neuroimages. Comput. Biomed. Res. 29, 162–173.
50. Talairach, J. and Tournoux, P. *Co-planar Steriotaxic Atlas of the Human Brain*. (1988). Thieme: New York.
51. Box, G.E., Jenkins, G.M., and Reinsel, G.C. *Time Series Analysis, Forecasting and Control.* (1994). Prentice Hall: Englewood Cliff, NJ.
52. Forman, S.D., Cohen, J.D., Fitzgerald, M., Eddy, W.F., Mintun, M.A., and Noll, D.C. (1995). Improved assessment of significant activation in functional magnetic resonance imaging (fMRI): use of a cluster-size threshold. Magn. Reson. Med. 33, 636–647.
53. Oldfield, R.C. (1971). The assessment and analysis of handedness: the Edinburgh inventory. Neuropsychologia 9, 97–113.
54. Raichle, M.E. and Mintun, M.A. (2006). Brain work and brain imaging. Annu. Rev. Neurosci. 29, 449–476.

55. McCrea, M., Guskiewicz, K.M., Marshall, S.W., Barr, W., Randolph, C., Cantu, R.C., Onate, J.A., Yang, J., and Kelly, J.P. (2003). Acute effects and recovery time following concussion in collegiate football players: the NCAA Concussion Study. JAMA 290, 2556–2563.
56. Schretlen, D.J. and Shapiro, A.M. (2003). A quantitative review of the effects of traumatic brain injury on cognitive functioning. Int. Rev. Psychiatry 15, 341–349.
57. Rosenbaum, S.B. and Lipton, M.L. (2012). Embracing chaos: the scope and importance of clinical and pathological heterogeneity in mTBI. Brain Imaging Behav. 6, 255–282.
58. Rasmussen, I.A., Xu, J., Antonsen, I.K., Brunner, J., Skandsen, T., Axelson, D.E., Berntsen, E.M., Lydersen, S., and Haberg, A. (2008). Simple dual tasking recruits prefrontal cortices in chronic severe traumatic brain injury patients, but not in controls. J. Neurotrauma. 25, 1057–1070.
59. Hua, J., Stevens, R.D., Huang, A.J., Pekar, J.J., and van Zijl, P.C. (2011). Physiological origin for the BOLD poststimulus undershoot in human brain: vascular compliance versus oxygen metabolism. J. Cereb. Blood Flow Metab. 31, 1599–1611.
60. Poser, B.A., van Mierlo, E., and Norris, D.G. (2011). Exploring the post-stimulus undershoot with spin-echo fMRI: implications for models of neurovascular response. Hum. Brain Mapp. 32, 141–153.
61. Ances, B.M., Liang, C.L., Leontiev, O., Perthen, J.E., Fleisher, A.S., Lansing, A.E., and Buxton, R.B. (2009). Effects of aging on cerebral blood flow, oxygen metabolism, and blood oxygenation level dependent responses to visual stimulation. Hum. Brain Mapp. 30, 1120–1132.
62. Fox, P.T., Raichle, M.E., Mintun, M.A., and Dence, C. (1988). Nonoxidative glucose consumption during focal physiologic neural activity. Science 241, 462–464.
63. Frackowiak, R.S. (1988). Clinical application of positron tomographic studies in cerebrovascular disease. Am. J. Physiol. Imaging 3, 24–25.
64. Barkhoudarian, G., Hovda, D.A., and Giza, C.C. (2011). The molecular pathophysiology of concussive brain injury. Clin. Sports Med. 30, 33–48.
65. Bellgowan, P.S., Bandettini, P.A., van Gelderen, P., Martin, A., and Bodurka, J. (2006). Improved BOLD detection in the medial temporal region using parallel imaging and voxel volume reduction. Neuroimage 29, 1244–1251.
66. Behzadi, Y. and Liu, T.T. (2005). An arteriolar compliance model of the cerebral blood flow response to neural stimulus. Neuroimage 25, 1100–1111.

Address correspondence to:
Andrew R. Mayer, PhD
The Mind Research Network
Pete and Nancy Domenici Hall
1101 Yale Boulevard NE
Albuquerque, NM 87106

E-mail: amayer@mrn.org